Wavelength dependence of coherently induced transparency in a Doppler-broadened cascade medium

S. Shepherd, D. J. Fulton, and M. H. Dunn
J. F. Allen Physics Research Laboratories, Department of Physics and Astronomy, University of St. Andrews, St. Andrews, Fife KY16 9SS, Scotland

(Received 8 May 1996; revised manuscript received 3 September 1996)

The effect of changing the coupling laser transition, and hence the wavelength, on the coherently induced transparency seen by a probe beam in a Doppler-broadened cascade electromagnetically induced transparency (EIT) configuration is studied experimentally and theoretically. The transparency of the vapor is shown to be an effect not just of EIT, but of the varying Autler-Townes splitting for each velocity group within the vapor. Consequently, the best overall transparency for Rabi splittings less than the Doppler width is not at the position of matched coupling and probe wavelengths, but for coupling wavelengths less than that of the probe. [S1050-2947(96)06912-0]

PACS number(s): 42.50.Gy, 42.50.Hz, 32.60.+i, 32.80.Qk

The coherent effect of an electromagnetically induced transparency (EIT) [1], and the related one of lasing without inversion (LWI) [2] have excited much attention over the last few years. In particular, there has been a great deal of work using rubidium vapor as an interaction medium in which effects can be observed while using cw laser sources [3–5]. In rubidium, the wavelengths involved in the most basic configurations of cascade, λ and V schemes are in the near infrared, and therefore easily covered by both diode and titanium sapphire laser sources. Also, since the wavelengths of probe and coupling lasers in these configurations are similar, the proper choice of co- or counterpropagating beams can reduce the Doppler-broadened vapor to a virtually Doppler-free medium. To date, all schemes in rubidium, including that of the first cw inversionless laser [6], have taken advantage of these Doppler-free schemes. It had been thought that the use of a Doppler-free medium was necessary to reduce the power requirement on the coupling laser before transparency was observable. In this paper we will show both theoretically and experimentally that this is in fact not the case. Instead, for cascade configurations, if the wavelength of the coupling laser is less than that of the probe, there is no disadvantage in using mismatched wavelengths. This point has been previously discussed theoretically in a paper by Geo-Banacloche *et al.* [7]. Within their theoretical analysis the authors show that it is advantageous for the observation of EIT if an atomic system is chosen such that the coupling field is lower in wavelength than that of the probe field. We extend this idea to the experimental regime where the wavelength mismatch between the two optical fields is of the order of hundreds of nanometers. In so doing a physical explanation is obtained and the relative roles of Autler-Townes splitting and EIT are highlighted, in order to emphasize that in a vapor the two cannot be treated separately. The significance of this work lies in the prospect of inducing cw inversionless gain in Doppler-broadened media where the coupling wavelength is not similar to that of the probe, allowing new wavelengths to be accessed.

Figure 1(a) shows a typical cascade scheme for observing EIT. In Fig. 1(b) are shown the actual rubidium energy levels used in the experiments described in this paper. In each case the probe wavelength is 780 nm, while the coupling wavelength can have either of the wavelengths 776 nm, 741 nm, or 572 nm. This allows the effect on the probe absorption of varying the coupling laser wavelength to be verified experimentally.

In a Doppler-broadened medium the EIT position [corresponding to two-photon resonance between $|1\rangle$ and $|3\rangle$ in Fig. 1(a)] shifts across the velocity groups, v, such that

$$\Delta_1=(k_1\pm k_2)v-\Delta_2, \quad \begin{cases} + & \text{for copropagating beams} \\ - & \text{for counterpropagating beams} \end{cases} \tag{1}$$

(where $k_1=1/\lambda_{pr}$, $k_2=1/\lambda_{coup}$, v=velocity of velocity group, Δ_1=detuning of probe from $|1\rangle-|2\rangle$ transition, Δ_2=detuning of coupling field from $|2\rangle-|3\rangle$ transition).

If the wave vectors k_1 and k_2 are the same in magnitude, and the beams are counterpropagating, as in two-photon spectroscopy, then the position of resonance is the same for all velocity groups, and the medium can be considered as Doppler free. In general, for real atomic systems, this is not

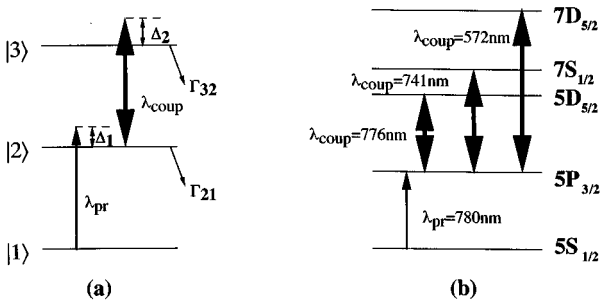

FIG. 1. (a) Schematic of a three-level atom for observing cascade EIT. Δ_1 is the detuning of the probe field from the $|1\rangle-|2\rangle$ resonance. Δ_2 is the detuning of the coupling field from the $|2\rangle-|3\rangle$ resonance. Γ_{32} is the population decay rate from $|3\rangle$ to $|2\rangle$, Γ_{21} is the population decay rate from $|2\rangle$ to $|1\rangle$. (b) Atomic levels in rubidium used for the three cascade systems explored in this paper. The probe is always fixed at 780 nm, while the coupling wavelength is varied to be resonant with different atomic transitions.

the case, and so any model which approximates an atomic vapor must take into account Doppler broadening. This integration over all velocity groups is standard procedure in the simulation of cw EIT effects in rubidium vapor [3,4,6], but a clearer idea of the physical processes involved in coherent transparency can be found by examining individual velocity groups, each of finite width, centered at different points across the Doppler profile. For each velocity group, the amount of transparency at the EIT point is set by the dephasing on the uncoupled transition γ_{13}, which in turn is determined by several factors, including the population decay from level $|3\rangle$ and the linewidth of the coherent sources used in the experiment [8]. Experimentally, this term is always greater than zero for cascade systems. If γ_{13} were zero, then the two-photon EIT position would be the point of maximum transparency for each velocity group. In reality this is not the case.

In addition to the effect of EIT on the probe absorption, the coupling field also induces Autler-Townes splitting of the levels $|2\rangle$ and $|3\rangle$, which are near resonance with the coupling field [9,10]. The absorption of the probe by any one atom, traveling with a velocity v will consequently split into two components separated by the generalized Rabi frequency $\tilde{\Omega}_R$ of the coupling laser. The transparency at any point between these two absorptions is also dependent on γ_{13}. The positions of the two absorptions change for each velocity group within the vapor and the overall probe absorption is the integral over all velocity groups.

The position of maximum transparency for any one velocity group is affected by both of the two effects described above; the interference EIT effect, and the Autler-Townes splitting effect. The magnitude of γ_{13} determines where the maximum transparency lies. For low γ_{13} values, the maximum transparency is near (or at, for $\gamma_{13}=0$) the EIT point, but the higher the dephasing, the less effective is the interference and the more the maximum transparency shifts to lie near the center of the two split levels. (In our model we have used a value of $\gamma_{13}=3.4$ MHz, consistent with our definitions based on the lifetimes of the relevant states within rubidium as outlined fully in Ref. [3]. For this dephasing value, the maximum transparency is still close to the two-photon point, as shown later.)

It is therefore important to ensure that the absorbing Autler-Townes components for any one velocity group do not overlap with the maximum transparency points of other velocity groups, as far as possible. We show that this tradeoff between absorptions and transparency across the velocity groups results in the best overall transparency occurring for wavelengths such that $\lambda_{coup}<\lambda_{pr}$, in the case where the Rabi frequency (Ω_R) is less than the Doppler width (ν_D), (as is usually the case for cw EIT experiments), and the dephasing term γ_{13} is greater than zero. Figure 2 shows the variation in the overall transparency at line center ($\Delta_1=\Delta_2=0$) vs coupling laser wavelength for two Rabi frequencies, given a fixed probe wavelength of 780 nm. This curve was calculated using a standard density-matrix analysis of the three-level system shown in Fig. 1(a) [3,11], with integration over all the velocity groups contributing to the probe Doppler width of ≈530 MHz full width at half maximum (FWHM). The shift in maximum transparency from where $\lambda_{coup}=\lambda_{pr}$ is clearly visible. The magnitude of this shift is dependent on

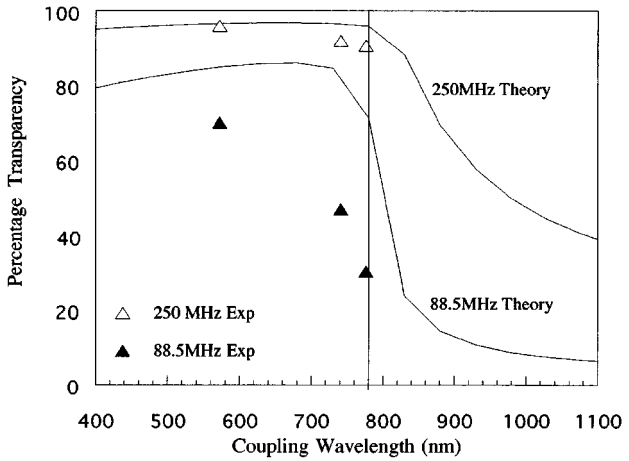

FIG. 2. Experimental and theoretical variation of percentage transparency vs coupling wavelength. Solid lines represent theoretical variation for $\Omega_{coup}=250$ MHz and $\Omega_{coup}=88.5$ MHz. Solid triangles represent experimental variation of $\Omega_{coup}=88.5$ MHz, open triangles represent experimental variation of $\Omega_{coup}=250$ MHz, each for $\lambda_{coup}=776$ nm, 741 nm, and 572 nm. The vertical line shown marks the position of matched wavelengths.

the value of the dephasing term γ_{13}, such that, provided $\gamma_{13}>0$, the best transparency will never be at $\lambda_{coup}=\lambda_{pr}$.

In order to assess the relative roles of EIT and Autler-Townes splitting in the overall induced transparency, the contribution of individual velocity groups is now considered. The frequency at which the probe experiences absorption due to the Autler-Townes split components of level $|2\rangle$ is affected by the velocity dependent detunings of both the coupling and probe fields. The prove field propagation direction is defined as always positive and the velocities of the atoms are positive if they move in the same direction. The coupling field propagates either co- or counter- to this direction. For a counterpropagating coupling beam the magnitude of the Autler-Townes splitting for each velocity group v is the generalized Rabi frequency for that group $\tilde{\Omega}_R$ and is related to the velocity dependent detuning of the coupling laser, $\Delta_2(v)$, such that,

$$\tilde{\Omega}_R=\sqrt{\Omega^2+[\Delta_2(v)]^2}=\left[\Omega^2+\left(\Delta_2+\frac{v}{\lambda_{coup}}\right)^2\right]^{1/2}, \quad (2)$$

where $\Omega=\mu E/\hbar$. (For copropagating coupling field use $-\lambda_{coup}$ instead of λ_{coup}.)

The center position of the two peaks is frequency shifted away from the unperturbed level $|2\rangle$ by an amount given by

$$-\frac{1}{2}\left(\Delta_2+\frac{v}{\lambda_{coup}}\right),$$

and the probe frequency is shifted by $-(v/\lambda_{pr})$. The overall effect of the three velocity dependent effects is that the probe is absorbed at frequencies around the uncoupled absorption position such that,

$$\nu_{\text{probe abs}}=\frac{v}{\lambda_{pr}}-\frac{1}{2}\left[\Delta_2+\frac{v}{\lambda_{coup}}\right]\pm\frac{1}{2}\left[\Omega^2+\left(\Delta_2+\frac{v}{\lambda_{coup}}\right)^2\right]^{1/2}. \quad (3)$$

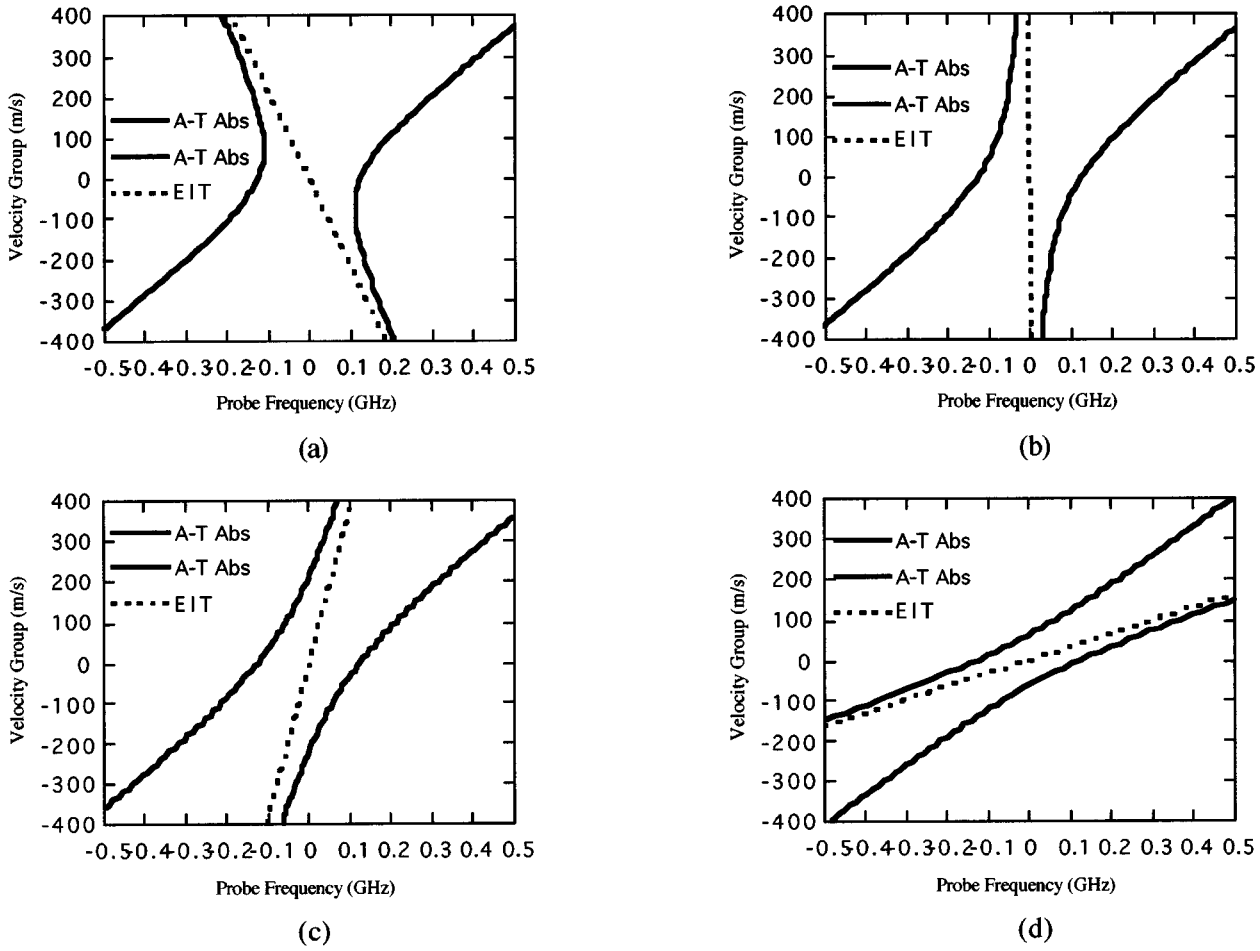

FIG. 3. Variation of frequency of Autler-Townes absorption components (solid lines) and EIT positions (dotted lines) vs probe frequency across the velocity groups. (a)–(c) are for counterpropagation to a probe wavelength of 780 nm with (a) $\lambda_{coup}=572$ nm, (b) $\lambda_{coup}=776$ nm, and (c) $\lambda_{coup}=980$ nm. (d) shows the case of $\lambda_{coup}=572$ nm copropagating with $\lambda_{probe}=780$ nm. The overlap of absorption with EIT across the velocity groups can be seen to get progressively worse from (a) to (d).

(For copropagating coupling field use $-\lambda_{coup}$ instead of λ_{coup}.)

The frequencies of the Autler-Townes split absorptions [described by Eq. (3)], and of EIT [described by Eq. (1)], as monitored by the probe, are shown in Fig. 3 as a function of the velocity groups. These are calculated for a probe wavelength of 780 nm, a coupling Rabi frequency of $\Omega_c=250$ MHz, and three different coupling wavelengths. Figure 3(a) shows the case of $\lambda_{coup}=572$ nm, given counterpropagating beams. It can be seen that there is a frequency region of 220 MHz around zero detuning in which there are no absorptions for any velocity group, but there is EIT. For $\lambda_{coup}=776$ nm [Fig. 3(b)] this region has shrunk to 62 MHz, and at $\lambda_{coup}=980$ nm is nonexistent. These graphs clearly show the advantage in having $\lambda_{coup}<\lambda_{probe}$, as the absorbing Autler-Townes components are shifted away from obscuring EIT, giving a better overall transparency region. Figure 3(d) shows the case of $\lambda_{coup}=572$ nm for co- instead of counter-propagating beams. The advantage of having a short coupling wavelength has now been lost, as the absorptions of one velocity group always encroach on the transparency of another velocity group. This graph does not change significantly for any coupling wavelength, showing why counter-propagating beams are the preferred geometry for observing transparency in a Doppler-broadened cascade medium.

Although Fig. 3 shows the positions of the Autler-Townes absorptions, the magnitude of each absorption also varies. The higher the velocity group the smaller are the absorptions of that group, due to the Doppler distribution. Also, for a particular group, the Autler-Townes component closer to the unperturbed position experiences more absorption. However, since the cascade scheme has a two-photon as well as the single-photon process contributing to the overall probe absorption, the weaker Autler-Townes component for each velocity group is still significant even at large shift frequencies [11]. A complete picture of the absorptions of the velocity groups is given for $\lambda_{coup}=776$ nm, $\Omega_c=250$ MHz in Fig. 4(a). The velocity groups are each 40 m/s wide and are shown by dotted lines, except for the group centered about zero velocity (-20 m/s$\rightarrow$20 m/s) which is marked by a thin solid line. The thick line represents the standard resultant over all velocity groups. Figure 4(b) is a closeup of the overlapping of the velocity bands near resonance, where the solid line corresponds to the group centered about zero velocity (-20 m/s$\rightarrow$20 m/s) as depicted previously by the thin solid line of Fig. 4(a). A dashed line is also included which simply

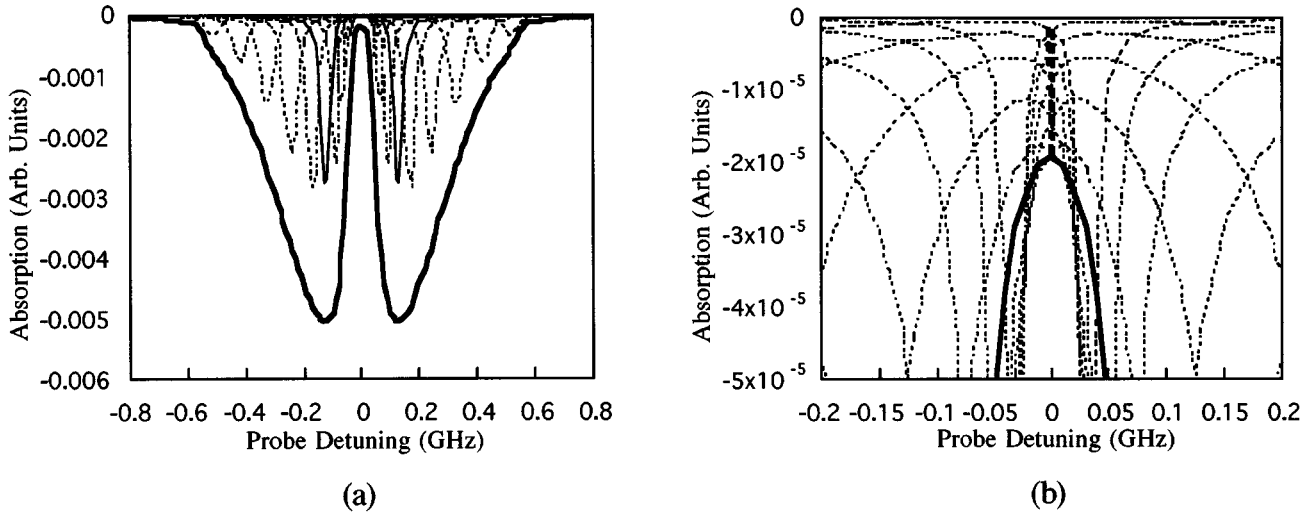

FIG. 4. (a) Variation of absorption of $\lambda_{pr}=780$ nm, for $\lambda_{coup}=776$ nm ($\Omega_{coup}=250$ MHz) with probe frequency for velocity groups 40 m/s wide spread across the Doppler profile. Each velocity group is marked by a dotted line, except for the group centered about zero velocity (-20 m/s$\rightarrow$20 m/s) which is marked by a thin solid line. The bold line shows the absorption for an integration over all velocity groups. (b) closeup of velocity groups shown in (a) at the resonance point. Solid line highlights the velocity group centered about zero velocity (-20 m/s$\rightarrow$20 m/s) and the dashed line connects the two-photon (EIT) positions of each velocity grouping.

connects the frequency positions of the two-photon EIT points of each velocity grouping. A similar picture for $\lambda_{coup}=572$ nm is given in Fig. 5. These pictures illustrate how, despite the position of maximum transparency (which is near the EIT position), shifting less with a velocity band for 776 nm than for 572 nm, the resultant is a deeper, wider transparency window in the latter case since the Autler-Townes absorptions are also shifted far away from the mid-resonance point for $\lambda_{coup}=572$ nm. In short, the absorptions in the 572 nm case do not erode into the transparency region as much as they do for longer coupling wavelengths. As previously discussed the idea that a negative residual Doppler width should enhance a transparency in cascade configurations was previously mentioned in the mathematical analysis of Geo-Banacloche *et al.* [7], but to date no experiments have been carried out in this region, and the role of Autler-Townes absorption in association with EIT as a means of reducing transparency has not been addressed.

The effect of varying the coupling laser wavelength on a transparency in cascade systems was examined experimentally by using the three rubidium transitions, $5P_{3/2}-5D_{5/2}$ (776 nm), $5P_{3/2}-7S_{1/2}$ (741 nm), and $5P_{3/2}-7D_{5/2}$ (572

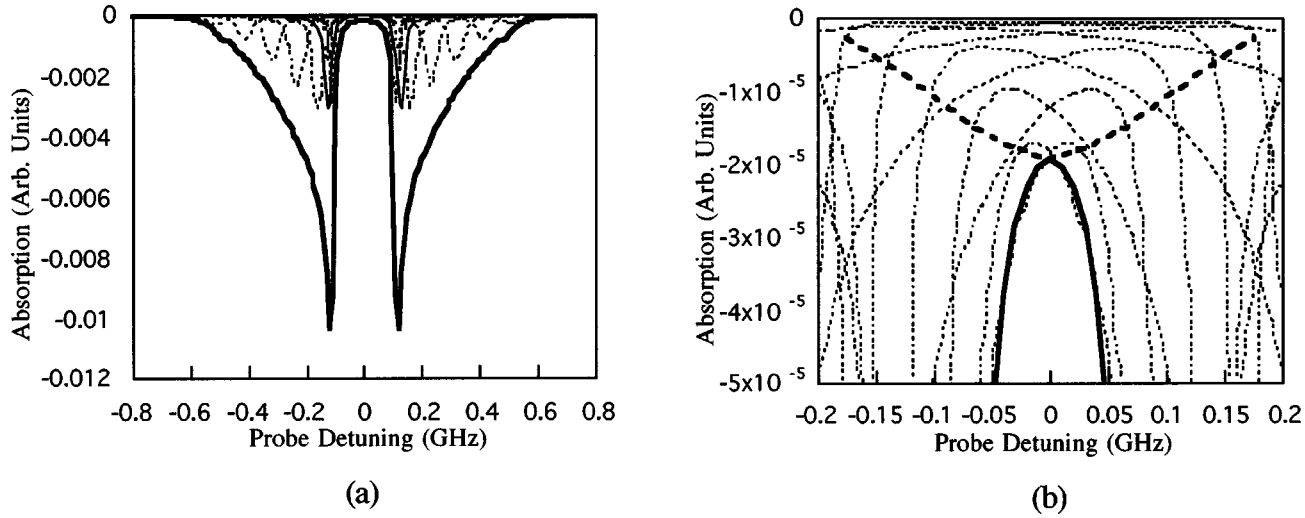

FIG. 5. (a) Variation of absorption of $\lambda_{pr}=780$ nm, for $\lambda_{coup}=572$ nm with probe frequency for velocity groups 40 m/s wide spread across the Doppler profile. Each velocity group is marked by a dotted line, except for the group centered about zero velocity (-20 m/s$\rightarrow$20 m/s) which is marked by a thin solid line. The bold line shows the absorption for an integration over all velocity groups. (b) closeup of velocity groups shown in (a) at the resonance point. Solid line highlights the velocity group centered about zero velocity (-20 m/s$\rightarrow$20 m/s) and the dashed line connects the two-photon (EIT) positions of each velocity grouping.

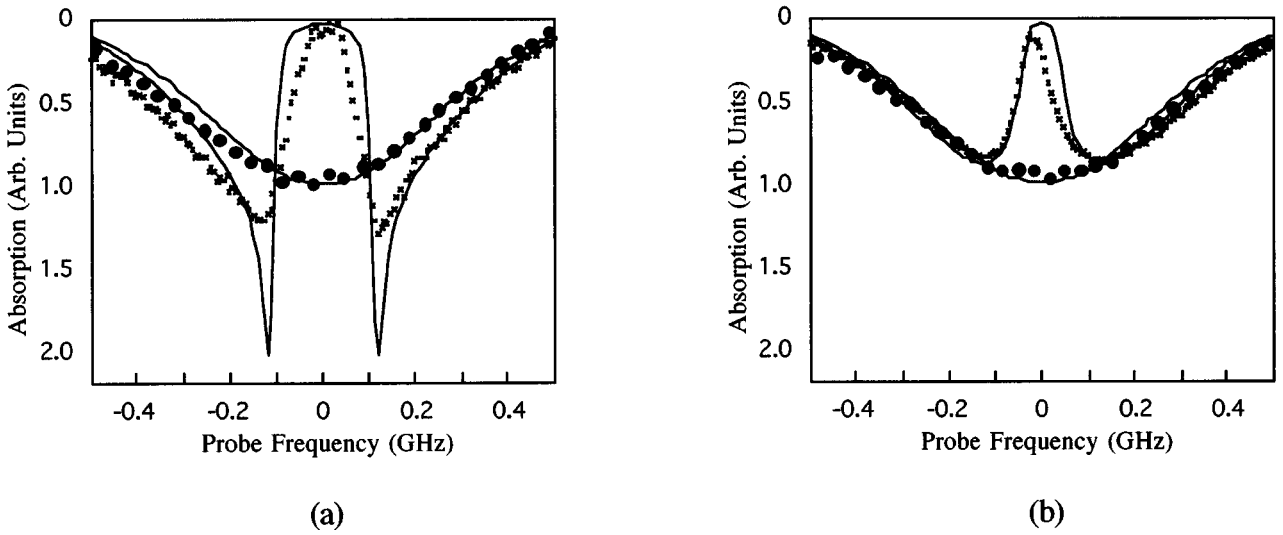

FIG. 6. Experimental absorption of 780 nm probe without (dots) and with (crosses) 250 MHz coupling laser, for (a) $\lambda_{coup}=572$ nm and (b) $\lambda_{coup}=776$ nm. Solid lines show theoretical fits to same parameters.

nm), as the coupling laser wavelengths. For each of these systems the probe laser wavelength was kept constant at 780 nm, corresponding to the $5S_{1/2}-5P_{3/2}$ transition. This wavelength was provided by a Microlase MBR110 scanning Ti:sapphire laser, with the output power filtered to 4 μw. The coupling laser wavelengths were provided by either a Schwartz Ti:sapphire or a Spectra-Physics 380D dye laser running on rhodamine 6G, depending on the wavelength required. The beams were all linearly polarized, and the polarizations of coupling and probe fields were parallel. As each transition has a different transition strength [12], the coupling laser intensity was varied to give equal rms Rabi frequencies on each transition. (There are a number of degenerate transitions excited by the coupling laser, with different Rabi frequencies, but the rms value is a fair indicator of the overall Rabi frequency.) This was done by satisfying the relation [13]

$$\Omega_{\rm rms}\propto\sqrt{\lambda^3 A\overline{\omega I}}=\text{const} \tag{4}$$

where λ=coupling laser wavelength (m), A=coupling transition strength (10^8/s), ϖ=degeneracy of upper level, I=Intensity (Wm^{-2}).

The probe was focused to a 50 μm waist within a 2 cm cell of rubidium vapor heated to 50 °C, and the coupling laser was focused to a waist of 135 μm. A wide area photodiode and phase-sensitive detector were used to detect the probe radiation. When on resonance with the $5S_{1/2}$ $(F=3)$ $-5P_{3/2}(F=4,3,2)$, ^{85}Rb transition, the absorption of the probe, in the absence of the coupling laser, was 60%.

Figure 6(a) shows the induced transparency on the probe for a coupling laser wavelength of 572 nm. The crosses and dots show the probe absorption in the presence and absence of the coupling laser. The solid lines show theoretical curves based on a Rabi frequency of 250 MHz. (This is in reasonably good agreement with the calculated Rabi frequency components for this transition. For the $m_J=3/2\rightarrow m_J=3/2$ and $m_J=1/2\rightarrow m_J=1/2$ transitions these are 273 and 343 MHz, respectively). Figure 6(b) shows the induced transparency on the probe for a coupling laser wavelength of 776 nm. There are two striking differences between Figs. 6(a) and 6(b). The first is that the frequency region of transparency for $\lambda_{coup}=572$ nm is larger than for $\lambda_{coup}=776$ nm and covers almost the entire range between the 250 MHz Autler-Townes split components of the $5P_{3/2}$ level. The second is the enhanced absorption on the wings of the transparency in the 572 nm case. Both features are experimentally quite obvious, though not as pronounced as expected, due probably to the range of Rabi frequencies present. (It is interesting to note that along with these features in the absorption spectrum, an increase in the variation of the dispersion of the probe for the case of $\lambda_{coup}=572$ nm is predicted, due to the increased transparency width. This will lead to stronger phaseonium [14] effects at lower coupling wavelengths.)

The experimental variation of an induced transparency with wavelength is shown by the triangles in Fig. 2, for the two different Rabi frequencies, 250 MHz and 88.5 MHz. The agreement is better at the higher Rabi frequency, where the blurring effect does not affect the maximum transparency, but the general trend of enhanced transparency at lower coupling wavelengths is obvious.

In conclusion, we have shown that a coherent transparency in a Doppler-broadened medium depends not just on the two-photon EIT position, but on the positions of the Autler-Townes components across the velocity groups. The position of maximum transparency for any one velocity group is determined by the amount of dephasing present, i.e., γ_{13}. The overall transparency is obtained by integrating over all the velocity groups. The amount of transparency for any individual velocity group is set by the dephasing, but the width is controlled by the Autler-Townes splitting. By trading off the Autler-Townes absorption positions against the maximum transparency position across the velocity groups, it is possible to increase overall transparency at low coupling powers by altering the coupling laser wavelength.

[1] K.-J. Boller, A. Immoğlu, and S. E. Harris, Phys. Rev. Lett. **66**, 2593 (1991).
[2] P. Mandel, Contemp. Phys. **34**, 235 (1993).
[3] D. J. Fulton, S. Shepherd, R. R. Moseley, B. D. Sinclair, and M. H. Dunn, Phys Rev. A. **52**, 2302 (1995).
[4] Y-q Li, S-z. Jin, and M. Xaio, Phys. Rev. A. **51**, R1754 (1995).
[5] A. Weiss, F. Sander, and S. I. Kanorsky, in *IEEE Technical Digest, Fifth European Quantum Electronics Conference 1994* (Optical Society of America, Washington, DC, 1994), p. 252.
[6] A. S. Zibrov, M. D. Lukin, D. E. Nikonov, L. Hollberg, M. O. Scully, V. L. Velichansky, and H. G. Robinson, Phys. Rev. Lett. **75**, 1499 (1995).
[7] J. Geo-Banacloche, Y-q Li, S-z Jin, and M. Xaio, Phys. Rev. A **51**, 576 (1995).
[8] B. J. Dalton and P. L. Knight, Opt. Commun. **42**, 411 (1982).
[9] P. L. Knight and P. W. Milonni, Phys. Rep. **66**, 21 (1980).
[10] H. R. Gray and C. R. Stroud, Jr., Opt. Commun. **25**, 359 (1978).
[11] R. R. Moseley, S. Shepherd, D. J. Fulton, B. D. Sinclair, and M. H. Dunn, Opt. Commun. **119**, 61 (1995).
[12] A. Lindgård and S. E. Nielsen, At. Data Nucl. Data Tables **19**, 606 (1977).
[13] B. Shore, *The Theory of Coherent Atomic Excitation* (Wiley, New York, 1990), Vol. 2.
[14] M. Fleischhauer, C. H. Keitel, M. O. Scully, C. Su, B. T. Ulrich, and S. Y. Zhu, Phys Rev. A **46**, 1468 (1992).